arXiv:2207.14425v1 [cs.CV] 29 Jul 2022

3D Cartoon Face Generation with Controllable Expressions from a Single GAN Image

Hao Wang, Guosheng Lin, Steven C. H. Hoi, *Fellow, IEEE* and Chunyan Miao

***Abstract*—In this paper, we investigate an open research task of generating 3D cartoon face shapes from single 2D GAN generated human faces and without 3D supervision, where we can also manipulate the facial expressions of the 3D shapes. To this end, we discover the semantic meanings of StyleGAN latent space, such that we are able to produce face images of various expressions, poses, and lighting by controlling the latent codes. Specifically, we first finetune the pretrained StyleGAN face model on the cartoon datasets. By feeding the same latent codes to face and cartoon generation models, we aim to realize the translation from 2D human face images to cartoon styled avatars. We then discover semantic directions of the GAN latent space, in an attempt to change the facial expressions while preserving the original identity. As we do not have any 3D annotations for cartoon faces, we manipulate the latent codes to generate images with different poses and lighting, such that we can reconstruct the 3D cartoon face shapes. We validate the efficacy of our method on three cartoon datasets qualitatively and quantitatively.**

***Index Terms*—3D Generation, Image Manipulation.**

I. Introduction

The Metaverse is a virtual world having persistent online computer-generated environments, where users in remote locations are able to interact in real time for the purpose of work or play through the Internet [1]. To this end, using the AI systems to construct high fidelity 3D environment is essential to the metaverse applications [2]. Various 3D reconstruction works [3]–[5] have been proposed to give solutions to automatically build the 3D world. Whereas translating 2D human faces into 3D personalized cartoon avatars remains challenging, since most of the existing works [6], [7] require rich multi-view 2D information or depth annotations, which are difficult to obtain massively. Moreover, to realize the synchronization between the 2D human faces and the 3D stylized avatars, we need to not only do the style transfer but also allow the 3D avatars to share the same expressions as the original human faces.

In this paper, we demonstrate a new application where we aim to generate 3D cartoon avatars based on single GAN generated human faces and without any 3D supervision. Here we do not need any annotations of the multi-view or the depth information. Specifically, our proposed task consists of two branches: one is to generate the stylized cartoon images given the GAN generated human face images, where we can manipulate the facial expressions; another one is to reconstruct the 3D shapes from single 2D images only. The main challenge of our proposed task is to realize the consistency between the 2D human faces, the 2D stylized cartoon faces, and the 3D reconstructed shapes. To this end, we bridge relationships between them through the StyleGAN [8] latent space $\mathcal{W}$, as is shown in Figure 1.

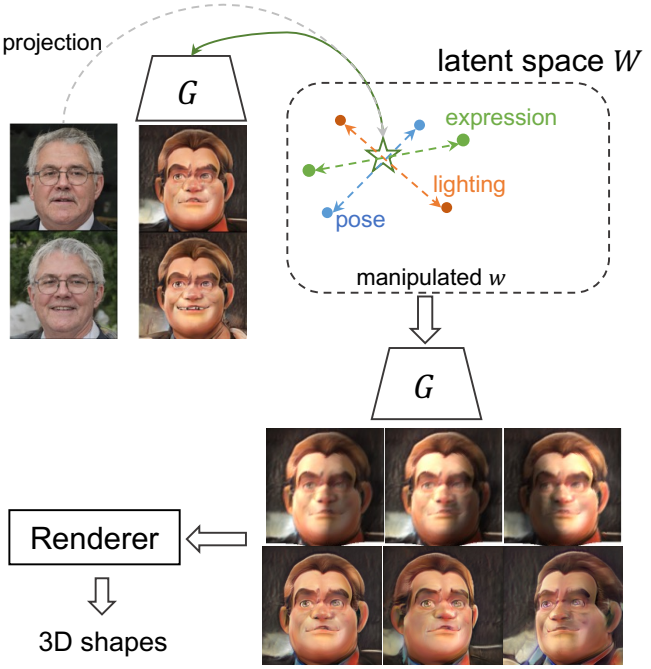


Fig. 1. Overview of our proposed pipeline. To this end, we train StyleGAN models for human faces and cartoon datasets respectively. Given a single GAN generated human face image, we first discover its corresponding latent codes $\mathbf{w}$ in the latent space $\mathcal{W}$, where we input $\mathbf{w}$ to the cartoon generator G and give the cartoon faces. We then aim to uncover the semantic directions of $\mathbf{w}$, by which we can manipulate the facial expressions, poses and lighting of the generated images. The manipulated images are fed into neural renderer for 3D reconstruction.

Previous works [8]–[11] have demonstrated that the disentanglement of StyleGAN latent space $\mathcal{W}$. That means we can manipulate the latent codes in space $\mathcal{W}$ to change one semantic attribute while preserving the other attributes. Therefore, the StyleGAN [8], [9] model can give images of the same person, but with various facial expressions, poses and lighting conditions.

As the preliminary of our proposed method, we assume the given human face images are generated from a StyleGAN model pretrained on FFHQ [9] dataset. If the input is a real-world face image, GAN inversion methods [8], [12]–[14] can be used to project the given face image back to the latent

Hao Wang, Guosheng Lin and Chunyan Miao are with School of Computer Science and Engineering, Nanyang Technological University. E-mail: {hao005,gslin,ascymiao}@ntu.edu.sg.

Steven C. H. Hoi is with Singapore Management University and Salesforce Research Asia. E-mail: chhoi@smu.edu.sg.

Corresponding authors: Chunyan Miao and Guosheng Lin.

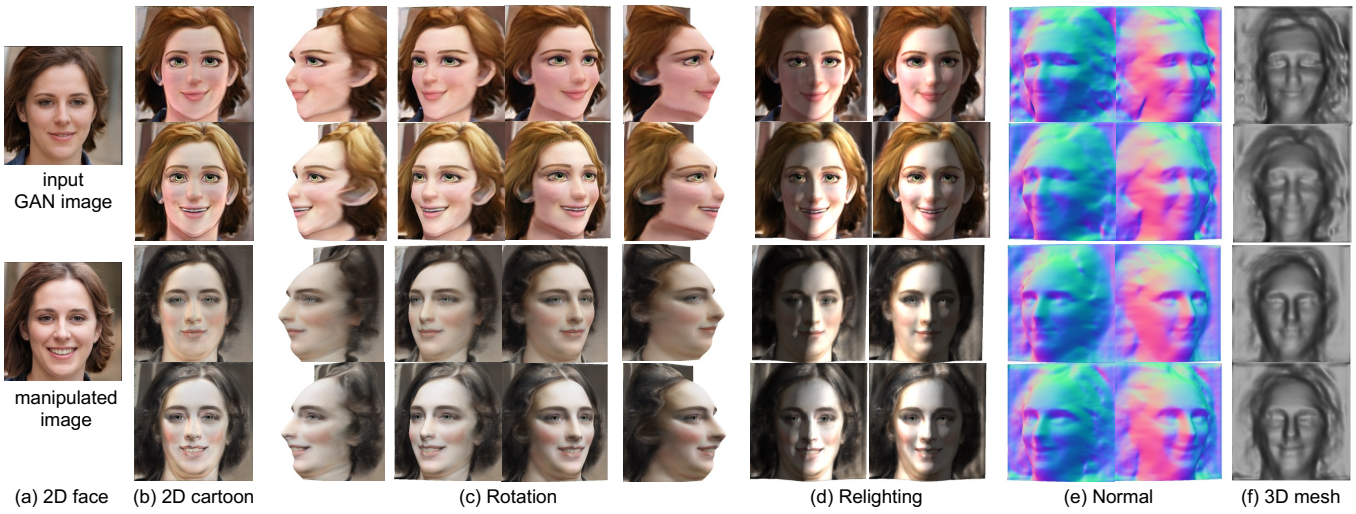


Fig. 2. In Column (a), input a GAN image, we can manipulate the input face image by changing the StyleGAN latent code. The corresponding generated cartoon styled images are presented Column (b). Column (c) and (d) present the rendered results of various viewpoints and lighting conditions. Column (e) and (f) show the normal maps and 3D mesh.

space $\mathcal{W}$ through the face generator, so that we can obtain the corresponding latent code. We then do the image-to-image translation to add cartoon style onto the original face images. To this end, we finetune the pretrained FFHQ model to train a cartoon face generation model. Specifically, we feed the same latent codes to both the FFHQ and cartoon generation models, and regularize the training through the output of the intermediate layers [15]. This allows these two generation models to share similar latent space $\mathcal{W}$, making the cartoon and human face images generated from the same latent codes have similar semantic attributes.

To manipulate the StyleGAN latent codes and give images with various facial expressions, we use closed-form factorization proposed in SeFa [10] to give the manipulated offsets for the latent codes. However, we find the initial offsets discovered by SeFa would also make some undesired semantic concepts changed, such as face identities and shapes, when modifying the facial expressions. To resolve this issue, we further optimize the initial offsets by the face identity loss and the low-level feature loss. As a result, we can get latent codes with expressions changed only. Based on the obtained latent codes, we then discover its variations for different poses and lighting conditions, which are used as the pseudo samples to reconstruct the 3D shapes.

Our contributions can be summarized as follows: (i) we propose a novel framework to generate 3D cartoon face shapes given single GAN generated human face images, which does not require any 3D supervision; (ii) we propose to generate 3D cartoon shapes with controllable expressions, where we optimize the manipulated latent code offsets, such that we can modify the facial expressions and keep other semantic attributes unchanged; and (iii) we show promising results both qualitatively and quantitatively, in which our model can generate high-quality 3D cartoon face shapes, with controllable facial expressions, poses, and lighting conditions.

II. Related Work

A. Image manipulation

Image manipulation [16], [17] aims to change the semantic attributes of the given images. Some works [11], [18] adopt the textual descriptions to manipulate images. Specifically, Wang et al. [11] use GAN inversion [14] to project the images back to the StyleGAN [9] latent space, and use paired image-text data to align the text embeddings with the GAN latent space, so that the images can be manipulated by the text features. To unsupervisedly discover meaningful latent directions of a pretrained GAN model, GANSpace [19] and SeFa [10] use Principal Component Analysis (PCA) to analyse the latent space. However, the discovered semantic directions by these methods are still coupled [20] with other semantic concepts. In our work, we propose to further optimize the directions found in SeFa, to make the manipulated face images change expressions only, while keeping other semantic attributes unchanged.

B. Image-to-image translation

Image-to-image translation (I2I) [21] aims to transfer images from a source domain to a target domain while preserving the representative contents [22]. I2I has been applied widely in various areas, including semantic image synthesis [23]–[25], style transfer [26], [27] and image inpainting [28]. Pix2Pix [29] adopts the conditional GAN architecture for the I2I task, however, it is only applicable on the paired datasets. To extend I2I to the unpaired datasets, many research works [27], [30], [31] are proposed for the unsupervised I2I learning. Although using cycle-consistent constraint [30] can give styles on the target images in the unpaired setting, it may not be feasible when dataset sizes of different domains are severely imbalanced [15]. To address this issue, Pinkney et al. [32] propose to finetune the StyleGAN model and use the method of "layer swapping" to produce photo-realistic images. Back

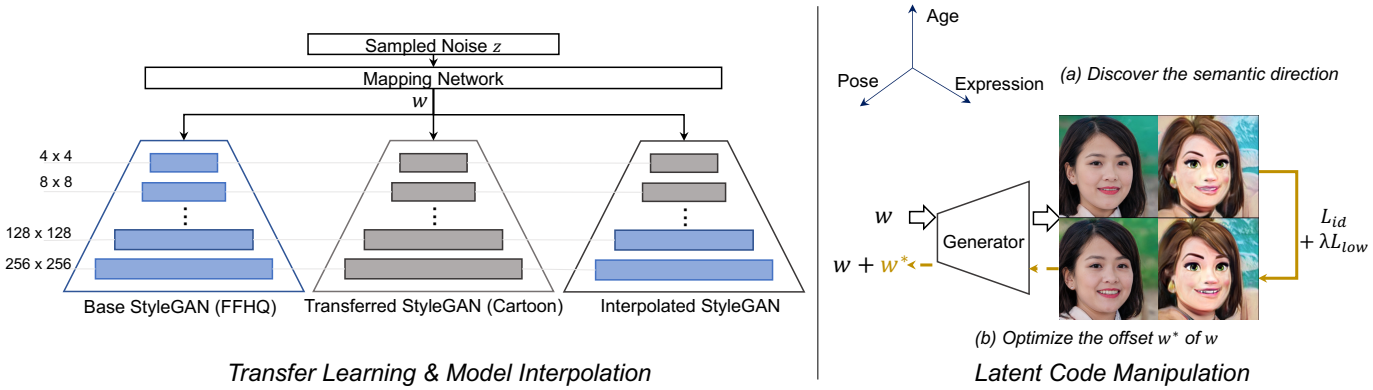


Fig. 3. The demonstration of the 2D cartoon face generation model training and latent code manipulation process. We first finetune the pretrained FFHQ StyleGAN model on the cartoon dataset. It is notable that we feed the same latent codes into the cartoon generator as that to the human face image generator. We then interpolate the transferred model, such that we can generate photo-realistic cartoon images. In the latent code manipulation phase, we first discover the semantic directions in the latent space $\mathcal{W}$ of the trained StyleGAN model. We then optimize the offset $\mathbf{w}^*$ to the original latent code $\mathbf{w}$ with the identity loss $\mathcal{L}_{id}$ and low-level feature regularization loss $\mathcal{L}_{low}$.

et al. [15] further improve the consistency between the original and stylized images by adding the regularization between the model intermediate outputs.

C. Unsupervised 3D shape learning

Since the 3D shape reconstruction requires images of consistent multiple views and lighting, recent works [6], [7], [20], [33], [34] attempt to uncover extra cues to guide the learning process. Kanazawa et al. [6] use an image collection under the same category as supervision to learn the reconstruction model. Wu et al. [34] takes an autoencoding pipeline, where they infer the depth, albedo, viewpoint and lighting from a single image, and use the reconstruction loss to supervise the training. [20], [33], [35] aim to manipulate the latent codes of StyleGAN [8], [9] to generate synthetic data for 3D shape learning. However, Zhang et al. [35] require the manual annotations for different views. Shi et al. [33] propose to train a 3D generator to disentangle the latent codes into 3D components, which are used as the input for the renderer. However, they [33] try to infer the depth information without any constraints from the latent codes, this may result in the estimated depth not being precise. Pan et al. [20] adopts an ellipsoid shape as the shape prior, giving better estimations on the face depth. Hence we follow [20] to reconstruct the 3D cartoon shapes.

III. Method

Our proposed framework for 3D cartoon face generation from single 2D GAN generated images is shown in Figure 3 and 4. The whole pipeline can be summarized as a three-stage learning scheme:

- **Stage 1.** We first finetune the pretrained FFHQ [9] StyleGAN model with the cartoon dataset. Then we interpolate the cartoon generation model weights to generate 2D photo-realistic cartoon faces.
- **Stage 2.** We aim to discover the semantic directions of the StyleGAN latent space $\mathcal{W}$. To manipulate one semantic concept only of the generated images, while keeping the face identity unchanged, we propose to optimize the offsets $\mathbf{w}^*$ with the identity loss $\mathcal{L}_{id}$ and the low-level feature regularization loss $\mathcal{L}_{low}$.
- **Stage 3.** Since StyleGAN can generate images of various poses and lighting conditions, we use it to give pseudo samples to reconstruct the 3D shapes of cartoon faces, which are generated based on the discovered original and manipulated latent codes. The iterative training scheme is utilized to improve the reconstructed results.

In the following sections, we give more technical details.

A. StyleGAN preliminaries

Prevailing generative adversarial networks (GANs) take the randomly sampled noise codes $\mathbf{z}$ as the input and produce fake images, which can be denoted as $G(\cdot) : \mathcal{Z} \rightarrow \mathcal{X}$. Karras et al. [8], [9] propose to map random noise $\mathbf{z} \in \mathcal{Z}$ to the latent code $\mathbf{w} \in \mathcal{W}$ with the Multi-Layer Perceptron (MLP). Recent works [8]–[11] demonstrate that the style-based generator can produce high-fidelity images, and the learned latent space $\mathcal{W}$ is disentangled with respect to various semantic attributes. This means we may manipulate the latent codes $\mathbf{w}$ and generate face images with different facial expressions, poses and lighting conditions, that are useful for the 3D shape reconstruction.

B. 2D cartoon generation model

As shown in the right column of Figure 3, we use transfer learning and the model interpolation [32] technique to train a StyleGAN model on the cartoon dataset. The reasons that we adopt the transfer learning technique have two folds: 1) the training samples are limited in some cartoon datasets and 2) we want the generated cartoon images to share similar semantic contents to the original face images, such as gender and facial expressions. Therefore, finetuning on a well-trained face StyleGAN model is an efficient way to realize the translation to the high-fidelity cartoon avatars [15], [36], [37].

To be specific, we take the StyleGAN model pretrained on FFHQ [9] as the base model, and finetune it on the cartoon

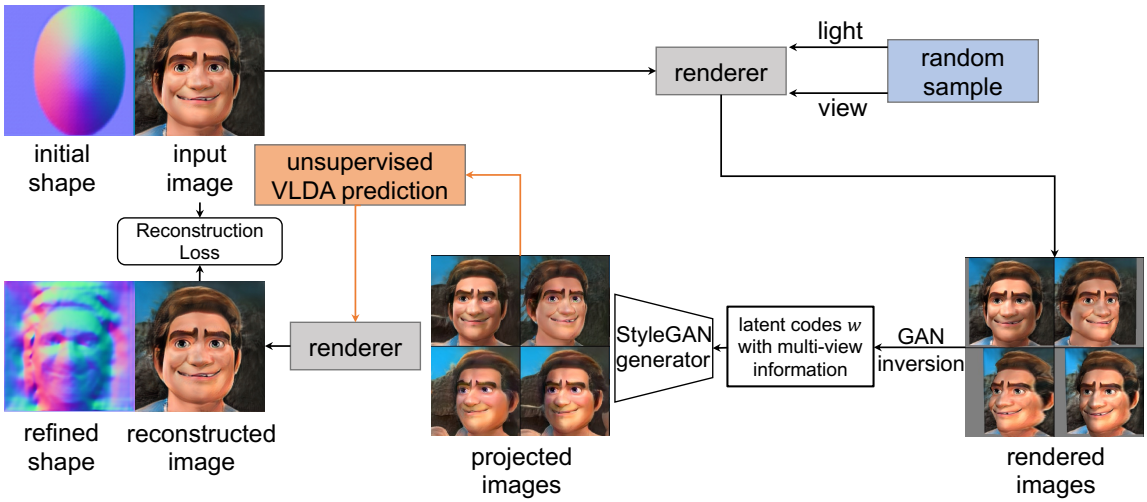


Fig. 4. The demonstration of 3D cartoon shape reconstruction process. VLDA stands for the viewpoint, lighting, depth and albedo respectively. Given an input image, we feed it into the renderer with the initial shape prior. We randomly sample lighting conditions and viewpoints, giving rendered images from various viewpoints and lighting. These rendered results from the 3D shapes are further projected back to the latent space $\mathcal{W}$ of StyleGAN. This gives better quality for the projected images, which are used to refine the initial shapes. The reconstruction loss is applied on the input and the reconstructed images.

datasets. During the finetuning process, other than using the adversarial training method on the transferred model, we also follow [15] to apply the structure loss between the base model and the transferred model. Technically, since StyleGAN takes the progressive generation strategy, we can obtain the generated images from various resolutions. To realize the trade-off between the generated cartoon styles and the original face semantics, we use the structure loss to make the low-resolution layer outputs of the base model and that of the transferred model be similar. The structure loss can be formulated as:

$$\mathcal{L}_{str} = \frac{1}{n}\sum_{k=1}^{n} ||G^k_{base}(\mathbf{z}) - G^k_{trans}(\mathbf{z})||^2, \tag{1}$$

where k denotes the index of the StyleGAN block, n represents we apply the structure loss on the first n blocks. G_{base} and G_{trans} refer to the base and transferred models respectively. It is notable that the weights of G_{base} are fixed. The adversarial loss is also utilized during finetuning, which can be denoted as:

$$\mathcal{L}_{adv} = \mathop{\mathbb{E}}_{\mathbf{x}\sim p_{data}}[\log D(\mathbf{x})] + \mathop{\mathbb{E}}_{\mathbf{z}\sim p_{\mathbf{z}}}\Big[\log\Big(1 - D\big(G_{trans}(\mathbf{z})\big)\Big)\Big]. \tag{2}$$

The overall objective for training the cartoon generation model is

$$\mathcal{L}_{gen} = \mathcal{L}_{adv} + \mathcal{L}_{str}. \tag{3}$$

We further adopt the model interpolation [32] technique to enable the interpolated StyleGAN model to produce more photo-realistic cartoon images. When we want to generate cartoon styled images that have similar semantics to the GAN generated human face images, we only need to feed the same latent codes $\mathbf{w}$ into the cartoon generator as that to the human face image generator.

C. Latent code manipulation

To control the semantic attributes, such as the facial expressions, of the generated avatars, we aim to discover the semantic directions of the StyleGAN latent space $\mathcal{W}$. Shen et al. [10] propose to use closed-form factorization to find the meaningful directions. To be specific, Shen et al. represent the transformation from the latent code $\mathbf{z}$ to $\mathbf{w}$ as

$$G_1(\mathbf{z}) \triangleq \mathbf{y} = \mathbf{A}\mathbf{z} + \mathbf{b}, \tag{4}$$

where $\mathbf{A}$ and $\mathbf{b}$ denote the weight and bias. Further, the manipulated latent codes are

$$G_1(\mathbf{z}') = G_1(\mathbf{z} + \alpha\mathbf{n}) = \mathbf{y} + \alpha\mathbf{A}\mathbf{n}, \tag{5}$$

where α indicates the manipulation intensity, and $\mathbf{n}$ denotes a certain direction in the latent space to represent a semantic attribute [10], [38]–[40]. As discussed in [10], the weight parameter $\mathbf{A}$ of the mapping network may contain the essential knowledge of the image variation. That means the latent semantic directions can be discovered by decomposing $\mathbf{A}$. To this end, we solve the following optimization problem

$$\mathbf{n}^* = \mathop{\arg\max}_{\{\mathbf{n}\in\mathbb{R}^d:\ \mathbf{n}^T\mathbf{n}=1\}} ||\mathbf{A}\mathbf{n}||_2^2, \tag{6}$$

where $||\cdot||_2$ indicates the l_2 norm.

However, we observe that manipulating the latent code with the discovered semantic direction $\mathbf{n}^*$ usually does not change one attribute only, while it may also affect some other semantic concepts, e.g. the face identity. To resolve this issue, we propose to optimize the offset $\mathbf{w}^*$ to the latent code. Technically, we use $\alpha\mathbf{n}^*$ as the initial offset. We then adopt a pre-trained face recognition network [33] $f(\cdot)$ to regularize the face identities, which can be denoted as

$$\mathcal{L}_{id} = ||f\big(G_{base}(\mathbf{w})\big) - f\big(G_{base}(\mathbf{w} + \mathbf{w}^*)\big)||^2. \tag{7}$$

Note that here we use the base StyleGAN model G_{base} for the optimization process, since there is no available cartoon face recognition network, and the transferred cartoon StyleGAN model has been trained to have similar latent space $\mathcal{W}$ to G_{base}.

To avoid getting trivial optimized results, where $\mathbf{w}^* \rightarrow 0$, we add another constraint to maximize the low-level features between the original and the manipulated face images. The low-level features captures more on the minor details and boundary information of faces. With a segmentation model [41], we feed the face areas only into the feature extractor $f_{low}(\cdot)$, which mitigates the background noise. The low-level feature regularization loss is

$$\mathcal{L}_{low} = ||f_{low}\big(G_{base}(\mathbf{w})\big) - f_{low}\big(G_{base}(\mathbf{w}+\mathbf{w}^*)\big)||^2. \quad (8)$$

The optimization objective can be formulated as

$$\mathcal{L}_m = \mathcal{L}_{id} - \lambda_{low}\mathcal{L}_{low}. \quad (9)$$

where λ_{low} is the trade-off hyper-parameter.

D. 3D shape reconstruction

We present the 3D reconstruction process from single 2D cartoon images in Figure 4. To reconstruct the 3D avatar shape from a single image, we follow the method proposed by [20], [34], where we use the manipulated images through StyleGAN to give the various viewpoint and lighting information. As indicated in Figure 4, the VLDA module (V, L, D, A) is needed to predict the viewpoint, lighting, depth and albedo respectively for the input images, which are constructed by different networks.

To be specific, we take the auto-encoding architecture. For a given image $\mathbf{I}$, we first predict its depth map $\boldsymbol{d}$, an albedo image $\boldsymbol{a}$, a viewpoint $\boldsymbol{v}$, and a light direction $\boldsymbol{l}$. With the above four factors, we can reconstruct the input images with the rendering process Φ:

$$\hat{\mathbf{I}} = \Phi(\boldsymbol{d}, \boldsymbol{a}, \boldsymbol{v}, \boldsymbol{l}), \quad (10)$$

where $\hat{\mathbf{I}}$ denotes the reconstructed images.

We take the iterative learning scheme of [20], and initialize the shape prior with an ellipsoid shape. In the first step, we use the canonical setting for the lighting and viewpoint conditions. We produce $\hat{\mathbf{I}}$ with the albedo network A and use the reconstruction loss between $\hat{\mathbf{I}}$ and $\mathbf{I}$ to train A, which are formulated as

$$\mathcal{L}_{recon} = ||\hat{\mathbf{I}} - \mathbf{I}|| + \lambda_{perc}||F(\hat{\mathbf{I}}) - F(\mathbf{I})||_2^2, \quad (11)$$

where the former and latter terms represent the L1 loss and the perceptual loss [42] respectively. $F(\cdot)$ denotes the VGG [43] feature extraction model.

In the second step, we randomly sample various viewpoints $\{\boldsymbol{v}_i | i = 1, 2, ..., m\}$ and lighting conditions $\{\boldsymbol{l}_i | i = 1, 2, ..., m\}$, which are used together with the depth $\boldsymbol{d}_0$ and albedo $\boldsymbol{a}_0$ that are computed at the first step to generate the rendered images. However, the rendered images have unnatural distortions, we follow [20] to project the rendered images back to the latent space $\mathcal{W}$ of StyleGAN, which gives strong regularization on the projected images, such that they can have better quality. Note that here we have the latent codes $\mathbf{w}$ for the original input images as discussed in Section III-C, hence we predict the offset $\Delta\mathbf{w}$ with an encoder $E(\cdot)$ to ease the training difficulty [20], whose optimization process can be denoted as

$$\mathcal{L}_E = \mathcal{L}_{dis}\Big(\mathbf{I}, G\big(E(\mathbf{I}) + \mathbf{w}\big)\Big) + \lambda_E \|E(\mathbf{I})\|_2. \quad (12)$$

$\mathcal{L}_{dis}$ denotes the L1 distance of discriminator features, which are demonstrated by [44] to be more useful at the generated samples. The latter term is used to avoid the learned offset being too large.

In the third step, we jointly train the V, L, D, A networks:

$$\begin{aligned}\mathcal{L}_{joint} =& \mathcal{L}_{recon}\Big(\tilde{\mathbf{I}}_i, \Phi\big(D(\mathbf{I}), A(\mathbf{I}), V(\tilde{\mathbf{I}}_i), L(\tilde{\mathbf{I}}_i)\big)\Big) \\ &+ \lambda_{smooth}\mathcal{L}_{smooth}\big(D(\mathbf{I})\big), \end{aligned} \quad (13)$$

which is the same way as [20]. Here $\tilde{\mathbf{I}}_i$ denotes the project sample, and $\mathcal{L}_{smooth}$ is defined in [45], which minimizes the L1 norm of the second-order gradients for the predicted depth maps. Training one cycle of the above three steps is not enough to reconstruct the 3D shape with fine details, hence we repeat these three steps four times to refine the 3D reconstructed results [20].

IV. Experiments

A. Setup

Datasets and metrics. We test our method on three cartoon face datasets: Disney [32], MetFaces [37] and Ukiyo-e [32]. Disney, MetFaces and Ukiyo-e contain 317, 1336 and 5209 images respectively. As these datasets do not have any ground-truth annotations for the 3D shapes, we evaluate the Fréchet Inception Distance (FID) [46] and perceptual loss $\mathcal{L}_{perc}$ [42] on the rendered 2D images from the 3D shapes.

Implementation details. We use the StyleGAN2 [8] model to train the cartoon datasets, which is based on the PyTorch implementation[1]. We apply the structure loss on the output of the first $n = 2$ blocks. For all of our used datasets, we resize the original images to the resolution of 256 and train the cartoon StyleGAN model. In the latent code manipulation process, we set the initial learning rate as 0.1 and the learning rate gradually decreases, which is the same strategy as used in [8]. For each sample, we optimize it for 10 iterations to give the w^*. We adopt the pretrained face embedding model used in [33] for $\mathcal{L}_{id}$ and $\mathcal{L}_{low}$, which is an ResNet-18 [47]. The structures of V, L, D, A networks are the same as [34]. Specifically, the depth and albedo networks are built by the encoder-decoder architecture, while viewpoint and lighting networks are implemented with encoders to give regressed results. We follow [20] to implement the GAN inversion encoder E, which uses the ResNet [47] architecture. The hyperparamters λ_{low}, λ_{perc}, λ_E and λ_{smooth} are set 0.2, 0.5, 0.01 and 0.01 respectively. The hyperparamters are chosen based on the empirical observations during model training.

B. Facial expression manipulation results

In Figure 5, we show the facial expression manipulation results across three different datasets, i.e. Disney [32], MetFaces [37] and Ukiyo-e [32]. We can see the overall consistency between the generated cartoon faces and the original human faces. To be specific, we first randomly sample latent codes of StyleGAN, where we further discover their semantic directions and present images with different facial expressions. The latent

[1]https://github.com/rosinality/stylegan2-pytorch



Fig. 5. Visualization of the manipulated facial expressions. In each block, from left to right, we show consistent results of natural human face images, Disney-style, Metfaces-style and Ukiyoe-style images respectively.

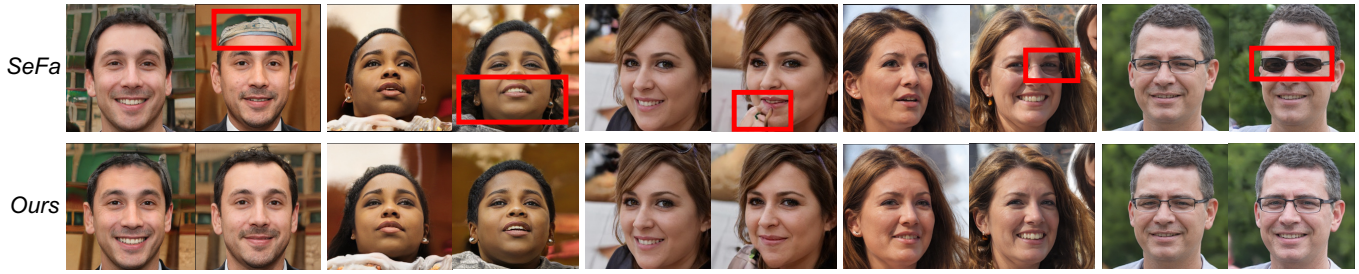


Fig. 6. Comparisons between SeFa [10] and our proposed latent code manipulation method. In each column, we show results generated by the manipulated latent codes, i.e. $\mathbf{w} + \mathbf{w}^*$ and $\mathbf{w} - \mathbf{w}^*$. The upper and bottom columns show images generated by SeFa [10] and our proposed method respectively. The red boxes depict the unwanted manipulated parts by SeFa [10], indicating our method can alleviate these issues.



Fig. 7. Visualization of image manipulation and cartoon style transferred results. We first manipulate the facial expressions of the GAN generated human face images, then we give the corresponding 2D cartoon avatars on three different datasets, which are shown in the top-right block. For ablation analysis, we further remove the structure loss and model interpolation respectively, and present the results on the bottom row.

TABLE I
QUANTITATIVE COMPARISONS ON FID AND PERCEPTUAL LOSS $\mathcal{L}_{perc}$ EVALUATED ON THE THREE DATASETS. WE ALSO GIVE ABLATION RESULTS TO ANALYZE THE USEFULNESS OF STRUCTURE LOSS AND MODEL INTERPOLATION.

Method	**Disney** [32]		**MetFaces** [37]		**Ukiyo-e** [32]	
Metrics	FID	$\mathcal{L}_{perc}$	FID	$\mathcal{L}_{perc}$	FID	$\mathcal{L}_{perc}$
Unsup3d [34]	205.6	0.71	192.5	0.71	316.8	0.73
LiftedGAN [33]	185.2	0.67	166.6	0.65	284.8	0.76
Ours	**146.8**	**0.65**	**140.7**	**0.64**	**188.1**	**0.71**
- w/o structure loss	159.9	0.65	156.9	0.70	280.3	0.75
- w/o model interpolation	181.7	0.70	189.5	0.64	234.0	0.72

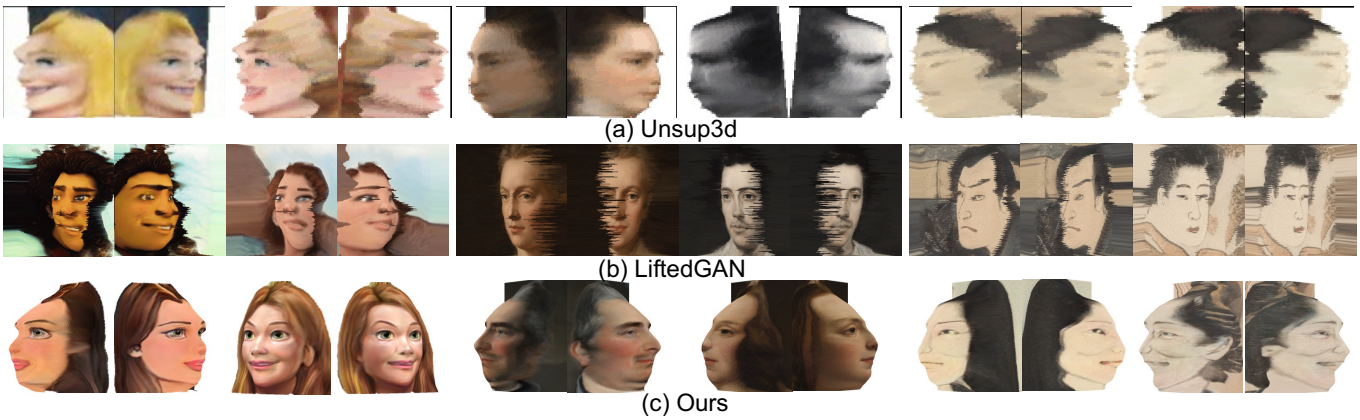


Fig. 8. Comparisons of qualitative results between ours and two related works: (a) Unsup3d [34] and (b) LiftedGAN [33].

codes that we feed into the cartoon StyleGAN model are the same as that in the human face model, hence the cartoon faces can share similar semantic concepts as the original human faces. For example, in the top-right block of Figure 5, our generated MetFaces-style and Ukiyoe-style cartoon faces have sunglasses, which do not exist in the original datasets but are consistent with the given human faces. Here we use SeFa [10] to find the initial offsets to manipulate the latent codes, then we propose to use the face identity loss and the low-level feature regularization loss to optimize the initial offsets.

C. Ablation studies

Efficacy of the latent code optimization. In Figure 6, we present the qualitative results of our proposed latent code manipulation method. We first follow SeFa [10] with the closed-form factorization method to find the semantic directions of the given latent codes $\mathbf{w}$, then we present images generated from the manipulated latent codes: $\mathbf{w}+\mathbf{w}^*$ and $\mathbf{w}-\mathbf{w}^*$. As shown in Figure 6, directly taking the $\mathbf{w}^*$ of SeFa [10] can change the facial expressions, while it fails to make other semantic concepts unchanged. For example, in the first column, the SeFa [10] manipulated image appears to have an unwanted bands around the head. Moreover, in the third column, SeFa [10] generated image has distortions around the chin. To resolve this issue, we propose to optimize $\mathbf{w}^*$ further with Eq. 9. It can be seen that faces optimized by our proposed method can not only keep the original face identity, but also give apparent facial expression variations.

Efficacy of the structure loss and model interpolation. In Figure 7, we present the visualizations of the image manipulation as well as the cartoon style transferred results. In each block, we generate cartoon faces with models trained with three different datasets. We observe the expressions of the transferred cartoon faces match with the original ones. For instance, in the top-right block, our method performs well at the Ukiyo-e dataset, where the training cartoon face data has few facial expression variations. When we remove model interpolation, we see the expression change is minor in these two datasets, as shown in the bottom row. Besides, it can also be observed that the structure loss helps generate more photo-realistic images, having better quality than images generated without structure loss.

D. Comparison with other works

Quantitative results. In Table I, we show the quantitative results of Unsup3d [34], LiftedGAN [33] and our proposed method. We also give ablative studies regarding the structure loss and model interpolation. For each dataset we sample 256 rendered 2D images for metrics calculation, and we use Fréchet Inception Distance (FID) [46] and the perceptual loss [42] $\mathcal{L}_{perc}$ to do the evaluation. To be specific, FID is to measure the distribution similarities between the rendered cartoon faces and the original FFHQ [9] datasets, and $\mathcal{L}_{perc}$ is to measure the instance similarity between cartoon and human faces. We observe our method performs better than Unsup3d [34] and LiftedGAN [33]. Specifically, model interpolation

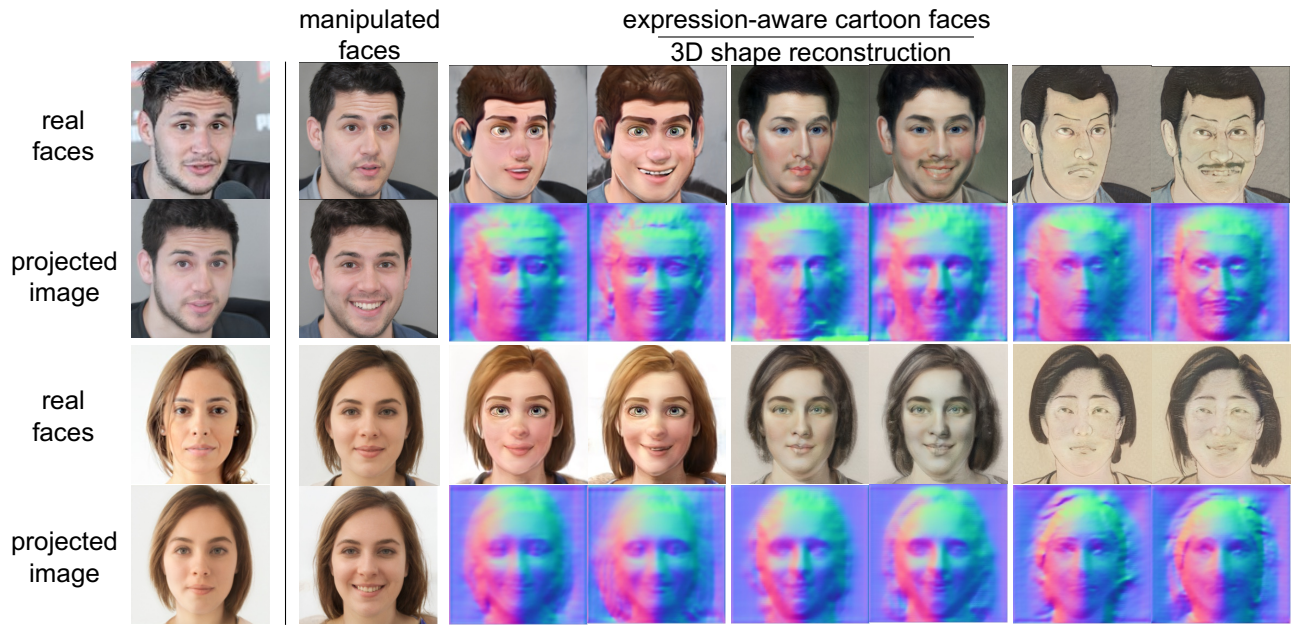


Fig. 9. Generated results from real face images. In the first column, we show the real faces and reconstructed images generated by the projected latent codes. In the second column, we show the faces with different facial expressions based on the manipulated latent codes. In the following columns, we show the cartoon faces and their reconstructed 3D shapes.

improves our results most, since it helps generate more photo-realistic cartoon images.

Qualitative results. In Figure 8, we show the rotated results of related works [33], [34] using the unsupervised method to reconstruct the 3D shapes. To be specific, we observe the 3D shapes reconstructed by Unsup3d [34] have unnatural distortions. Besides, as the rendered image size of Unsup3d is set as 64, the results also lack fine-grained details. Both LiftedGAN [33] and our method set the resolution as 256. LiftedGAN [33] performs well at generating the front cartoon faces only, while at other viewpoints, it renders low-quality images with large distortions, since LiftedGAN simply infers the depth from latent codes and trains the model without any constraint on the depth. In contrast, we initialize the shape prior with an ellipsoid shape and refine the reconstructed 3D shapes with multiple cycles, hence we can obtain results with better quality.

E. Applications on real human faces

In our previous experiments, we directly sample random latent codes $\mathbf{w}$ to generate human faces and cartoon avatars. If one wants to experiment with the real face data, existing GAN inversion methods [8], [12]–[14] can be used to project the real face images back to the latent space $\mathcal{W}$ and obtain the latent codes $\mathbf{w}$. This means in GAN inversion, we aim to find $\mathbf{w}$ that can reconstruct the given image with the trained GAN. Here we directly take the image projection method given by the StyleGAN2 implementation[2], we show the qualitative results in Figure 9. It is notable that better GAN inversion results can be expected if more advanced methods are adopted. Generally, we observe our method gives good manipulation and 3D reconstruction results.

[2]https://github.com/rosinality/stylegan2-pytorch

F. 3D shape reconstruction

In Figure 10, we show the visualizations from the 2D human faces to the learned 3D shapes. To be specific, we first aim to obtain the stylized cartoon faces, where we feed the same latent codes to the cartoon generation model as that of human faces. We show results of three cartoon datasets. The shown rotation and relighting results are rendered from the reconstructed 3D shapes. Generally, our framework can capture the fine-grained details of the 2D images, e.g. the face wrinkles and skin color. Moreover, the predicted eye directions are changed according to the rotation degrees. The surface normal map is used to generate face images with arbitrary lighting conditions. The relighting samples preserve the original face information with only lighting changed, indicating the quality of our learned normal maps. We also observe the reconstructed 3D mesh can reflect the hair texture, as shown in the fourth row.

G. Limitations

Our experimental results have demonstrated the proposed framework is able to generate 3D cartoon face shapes from the 2D images in an unsupervised manner. However, when the viewpoints have large rotation degrees, our reconstructed shapes may have unnatural distortions and miss fine-grained texture around the jaw, as shown in the last row of Figure 10. This is because that the StyleGAN fails to infer the images with various viewpoints correctly, as the original cartoon datasets may not provide enough diversity. Moreover, our proposed latent code optimization method can alleviate



Fig. 10. Visualization of our reconstructed expression-aware 3D shapes from the 2D human faces and without 3D supervision. From left to right, we first show the input and manipulated human face images, then the stylized cartoon faces of three datasets. Based on single cartoon face images, we learn its corresponding 3D shapes. We present results of rotations, relighting, surface normal and 3D mesh respectively.

the issue of SeFa [10] to some extent, but it appears to be challenging to change only one semantic attribute on the manipulated faces. For example, in the last column of Figure 6, our method can change the facial expressions and preserve the face identity, however, the hair color is also changed, since we only put a constraint on the face identity. To overcome the limitations, we can study more effective algorithms to improve the disentanglement of StyleGAN.

V. Conclusions

This paper presents a novel framework for the expression-aware 3D cartoon face shape generation from a single GAN generated human face image, where we do not need 3D supervision. Specifically, our framework takes the advantage of the disentanglement of StyleGAN latent space, where we manipulate the latent codes to generate images with various facial expressions, poses and lighting conditions. We propose to optimize the manipulated offsets of the latent codes to make only one semantic attribute changed and preserve other attributes. To stylize the given human face images, we first discover the corresponding latent codes of human faces, which are fed into the cartoon face generation model to give cartoon styled faces. We use the model interpolation technique to make the generated cartoon images more photo-realistic. During the 3D shape reconstruction process, we also manipulate the latent codes to give pseudo samples of different viewpoints and lighting conditions to enable 3D learning. The experimental results demonstrate the efficacy of our proposed framework in the 3D cartoon face generation and manipulation.

Acknowledgments

This research is supported, in part, by the National Research Foundation (NRF), Singapore under its AI Singapore Programme (AISG Award No: AISG-GC-2019-003) and under its NRF Investigatorship Programme (NRFI Award No. NRF-NRFI05-2019-0002). Any opinions, findings and conclusions or recommendations expressed in this material are those of the authors and do not reflect the views of National Research Foundation, Singapore. This research is supported, in part, by the Singapore Ministry of Health under its National Innovation Challenge on Active and Confident Ageing (NIC Project No. MOH/NIC/HAIG03/2017). This research is also supported by the National Research Foundation, Singapore under its AI Singapore Programme (AISG Award No: AISG-RP-2018-003), and the MOE AcRF Tier-1 research grant: RG95/20.

References

[1] J. D. N. Dionisio, W. G. B. III, and R. Gilbert, "3d virtual worlds and the metaverse: Current status and future possibilities," *ACM Computing Surveys (CSUR)*, vol. 45, no. 3, pp. 1–38, 2013.

[2] W. C. Ng, W. Y. B. Lim, J. S. Ng, Z. Xiong, D. Niyato, and C. Miao, "Unified resource allocation framework for the edge intelligence-enabled metaverse," *arXiv preprint arXiv:2110.14325*, 2021.

[3] M. Niemeyer and A. Geiger, "Giraffe: Representing scenes as compositional generative neural feature fields," in *Proceedings of the IEEE/CVF Conference on Computer Vision and Pattern Recognition*, 2021, pp. 11 453–11 464.

[4] S. Peng, Y. Zhang, Y. Xu, Q. Wang, Q. Shuai, H. Bao, and X. Zhou, "Neural body: Implicit neural representations with structured latent codes for novel view synthesis of dynamic humans," in *Proceedings of the IEEE/CVF Conference on Computer Vision and Pattern Recognition*, 2021, pp. 9054–9063.

[5] K. Schwarz, Y. Liao, M. Niemeyer, and A. Geiger, "Graf: Generative radiance fields for 3d-aware image synthesis," *arXiv preprint arXiv:2007.02442*, 2020.

[6] A. Kanazawa, S. Tulsiani, A. A. Efros, and J. Malik, "Learning category-specific mesh reconstruction from image collections," in *Proceedings of the European Conference on Computer Vision (ECCV)*, 2018, pp. 371–386.

[7] S. Tulsiani, A. A. Efros, and J. Malik, "Multi-view consistency as supervisory signal for learning shape and pose prediction," in *Proceedings of the IEEE conference on computer vision and pattern recognition*, 2018, pp. 2897–2905.

[8] T. Karras, S. Laine, M. Aittala, J. Hellsten, J. Lehtinen, and T. Aila, "Analyzing and improving the image quality of StyleGAN," in *Proc. CVPR*, 2020.

[9] T. Karras, S. Laine, and T. Aila, "A style-based generator architecture for generative adversarial networks," in *Proceedings of the IEEE/CVF Conference on Computer Vision and Pattern Recognition*, 2019, pp. 4401–4410.

[10] Y. Shen and B. Zhou, "Closed-form factorization of latent semantics in gans," in *Proceedings of the IEEE/CVF Conference on Computer Vision and Pattern Recognition*, 2021, pp. 1532–1540.

[11] H. Wang, G. Lin, S. C. Hoi, and C. Miao, "Cycle-consistent inverse gan for text-to-image synthesis," in *Proceedings of the 29th ACM International Conference on Multimedia*, 2021, pp. 630–638.

[12] J.-Y. Zhu, P. Krähenbühl, E. Shechtman, and A. A. Efros, "Generative visual manipulation on the natural image manifold," in *European conference on computer vision*. Springer, 2016, pp. 597–613.

[13] D. Bau, H. Strobelt, W. Peebles, B. Zhou, J.-Y. Zhu, A. Torralba *et al.*, "Semantic photo manipulation with a generative image prior," *arXiv preprint arXiv:2005.07727*, 2020.

[14] J. Zhu, Y. Shen, D. Zhao, and B. Zhou, "In-domain gan inversion for real image editing," in *Proceedings of European Conference on Computer Vision (ECCV)*, 2020.

[15] J. Back, "Fine-tuning stylegan2 for cartoon face generation," *arXiv preprint arXiv:2106.12445*, 2021.

[16] N. Yang, Z. Zheng, M. Zhou, X. Guo, L. Qi, and T. Wang, "A domain-guided noise-optimization-based inversion method for facial image manipulation," *IEEE Transactions on Image Processing*, vol. 30, pp. 6198–6211, 2021.

[17] F.-E. Yang, J.-C. Chang, C.-C. Tsai, and Y.-C. F. Wang, "A multi-domain and multi-modal representation disentangler for cross-domain image manipulation and classification," *IEEE Transactions on Image Processing*, vol. 29, pp. 2795–2807, 2019.

[18] H. Dong, S. Yu, C. Wu, and Y. Guo, "Semantic image synthesis via adversarial learning," in *Proceedings of the IEEE International Conference on Computer Vision*, 2017, pp. 5706–5714.

[19] E. Härkönen, A. Hertzmann, J. Lehtinen, and S. Paris, "Ganspace: Discovering interpretable gan controls," *arXiv preprint arXiv:2004.02546*, 2020.

[20] X. Pan, B. Dai, Z. Liu, C. C. Loy, and P. Luo, "Do 2d gans know 3d shape? unsupervised 3d shape reconstruction from 2d image gans," *arXiv preprint arXiv:2011.00844*, 2020.

[21] F. Gao, X. Xu, J. Yu, M. Shang, X. Li, and D. Tao, "Complementary, heterogeneous and adversarial networks for image-to-image translation," *IEEE Transactions on Image Processing*, vol. 30, pp. 3487–3498, 2021.

[22] Y. Pang, J. Lin, T. Qin, and Z. Chen, "Image-to-image translation: Methods and applications," *arXiv preprint arXiv:2101.08629*, 2021.

[23] K. Regmi and A. Borji, "Cross-view image synthesis using conditional gans," in *Proceedings of the IEEE Conference on Computer Vision and Pattern Recognition*, 2018, pp. 3501–3510.

[24] T. Park, M.-Y. Liu, T.-C. Wang, and J.-Y. Zhu, "Semantic image synthesis with spatially-adaptive normalization," in *Proceedings of the IEEE/CVF Conference on Computer Vision and Pattern Recognition*, 2019, pp. 2337–2346.

[25] P. Zhu, R. Abdal, Y. Qin, and P. Wonka, "Sean: Image synthesis with semantic region-adaptive normalization," in *Proceedings of the IEEE/CVF Conference on Computer Vision and Pattern Recognition*, 2020, pp. 5104–5113.

[26] T. Kim, M. Cha, H. Kim, J. K. Lee, and J. Kim, "Learning to discover cross-domain relations with generative adversarial networks," in *International Conference on Machine Learning*. PMLR, 2017, pp. 1857–1865.

[27] Z. Yi, H. Zhang, P. Tan, and M. Gong, "Dualgan: Unsupervised dual learning for image-to-image translation," in *Proceedings of the IEEE international conference on computer vision*, 2017, pp. 2849–2857.
[28] D. Pathak, P. Krahenbuhl, J. Donahue, T. Darrell, and A. A. Efros, "Context encoders: Feature learning by inpainting," in *Proceedings of the IEEE conference on computer vision and pattern recognition*, 2016, pp. 2536–2544.
[29] P. Isola, J.-Y. Zhu, T. Zhou, and A. A. Efros, "Image-to-image translation with conditional adversarial networks," in *Proceedings of the IEEE conference on computer vision and pattern recognition*, 2017, pp. 1125–1134.
[30] J.-Y. Zhu, T. Park, P. Isola, and A. A. Efros, "Unpaired image-to-image translation using cycle-consistent adversarial networks," in *Proceedings of the IEEE international conference on computer vision*, 2017, pp. 2223–2232.
[31] Y. Taigman, A. Polyak, and L. Wolf, "Unsupervised cross-domain image generation," *arXiv preprint arXiv:1611.02200*, 2016.
[32] J. N. Pinkney and D. Adler, "Resolution dependent gan interpolation for controllable image synthesis between domains," *arXiv preprint arXiv:2010.05334*, 2020.
[33] Y. Shi, D. Aggarwal, and A. K. Jain, "Lifting 2d stylegan for 3d-aware face generation," in *Proceedings of the IEEE/CVF Conference on Computer Vision and Pattern Recognition*, 2021, pp. 6258–6266.
[34] S. Wu, C. Rupprecht, and A. Vedaldi, "Unsupervised learning of probably symmetric deformable 3d objects from images in the wild," in *Proceedings of the IEEE/CVF Conference on Computer Vision and Pattern Recognition*, 2020, pp. 1–10.
[35] Y. Zhang, W. Chen, H. Ling, J. Gao, Y. Zhang, A. Torralba, and S. Fidler, "Image gans meet differentiable rendering for inverse graphics and interpretable 3d neural rendering," *arXiv preprint arXiv:2010.09125*, 2020.
[36] S. Mo, M. Cho, and J. Shin, "Freeze the discriminator: a simple baseline for fine-tuning gans," *arXiv preprint arXiv:2002.10964*, 2020.
[37] T. Karras, M. Aittala, J. Hellsten, S. Laine, J. Lehtinen, and T. Aila, "Training generative adversarial networks with limited data," *arXiv preprint arXiv:2006.06676*, 2020.
[38] L. Goetschalckx, A. Andonian, A. Oliva, and P. Isola, "Ganalyze: Toward visual definitions of cognitive image properties," in *Proceedings of the IEEE/CVF International Conference on Computer Vision*, 2019, pp. 5744–5753.
[39] Y. Shen, J. Gu, X. Tang, and B. Zhou, "Interpreting the latent space of gans for semantic face editing," in *Proceedings of the IEEE/CVF Conference on Computer Vision and Pattern Recognition*, 2020, pp. 9243–9252.
[40] C. Yang, Y. Shen, and B. Zhou, "Semantic hierarchy emerges in deep generative representations for scene synthesis," *International Journal of Computer Vision*, vol. 129, no. 5, pp. 1451–1466, 2021.
[41] C. Yu, J. Wang, C. Peng, C. Gao, G. Yu, and N. Sang, "Bisenet: Bilateral segmentation network for real-time semantic segmentation," in *Proceedings of the European conference on computer vision (ECCV)*, 2018, pp. 325–341.
[42] J. Johnson, A. Alahi, and L. Fei-Fei, "Perceptual losses for real-time style transfer and super-resolution," in *European conference on computer vision*. Springer, 2016, pp. 694–711.
[43] K. Simonyan and A. Zisserman, "Very deep convolutional networks for large-scale image recognition," *arXiv preprint arXiv:1409.1556*, 2014.
[44] X. Pan, X. Zhan, B. Dai, D. Lin, C. C. Loy, and P. Luo, "Exploiting deep generative prior for versatile image restoration and manipulation," *IEEE Transactions on Pattern Analysis and Machine Intelligence*, 2021.
[45] T. Zhou, M. Brown, N. Snavely, and D. G. Lowe, "Unsupervised learning of depth and ego-motion from video," in *Proceedings of the IEEE conference on computer vision and pattern recognition*, 2017, pp. 1851–1858.
[46] M. Heusel, H. Ramsauer, T. Unterthiner, B. Nessler, and S. Hochreiter, "Gans trained by a two time-scale update rule converge to a local nash equilibrium," *arXiv preprint arXiv:1706.08500*, 2017.
[47] K. He, X. Zhang, S. Ren, and J. Sun, "Deep residual learning for image recognition," in *Proceedings of the IEEE conference on computer vision and pattern recognition*, 2016, pp. 770–778.